

Predictive Current Control in Active Power Factor Correction Controller

Bello N.^{1*} and Edegbe E.¹

¹Department of Electrical and Electronic Engineering, Faculty of Engineering, University of Benin, PMB 1154, Benin City, Nigeria.

*Corresponding Author Email: nosabello@uniben.edu

Article Info

Keywords:

Harmonics, frequency, Distortion, Switching

Received 10 Sept. 2021

Revised 28 Sept. 2021

Accepted 30 Sept. 2021

Available online 10 June 2022



<https://doi.org/10.37933/nipes.e/4.2.2022.9>

<https://nipesjournals.org.ng>

© 2022 NIPES Pub. All rights reserved.

Abstract

The half-bridge (HB) LLC resonant converter is widely used in high and medium power applications, because of several advantages such as zero-voltage-switching (ZVS) capability over a wide input range and low component count. Most LLC resonant converters employ frequency modulation scheme to regulate the output power. However, in wide input voltage applications with widely varying hold-up time requirement, large switching losses are incurred during low power applications, which results in a low overall efficiency. A variable magnetizing inductance has been proposed for certain applications. However, this is not easy to implement as the relationship is not linear. This paper proposes a high efficiency, high power density half-bridge LLC resonant converter at low power application. High efficiency is reached at all power levels by introducing an operating mode: Low-power mode. Here, the output power is regulated by adjusting the voltage across the primary resonant capacitor. This provides for accurate mode control and linear power control. This method provides flexibility and ease of design for applications with largely varying power level requirement.

1 Introduction

Electrical Power Factor Correction (PFC) helps to reduce low order harmonics and improve the power factor to near unity without any alteration of the initial load. Comparing this method to the conventional two stage diode bridge rectifier [1]. The tracking capability required to follow precisely a rectified sinusoidal current reference is the major challenge of this method. There are several proposed methods for current control in PFC circuits including linear [2], hysteresis, sliding mode, and other non-linear control methods [3]. New technologies in PFC, like multistage PFC [4], interleaved boost PFC, flyback boost PFC, and three phase PFC [5], require a highly efficient controller in order to achieve a proper operating condition and near unity power factor. Alternative circuits and control schemes have been proposed to improve its efficiency when a high switching frequency is required [6].

In order to evaluate predictive control as an alternative to control a PFC rectifier, one classical input current control method-linear control is compared with predictive control method.

Linear control can be implemented using analog circuitry, but the gain adjustment and a large number of components implies larger cost and weight and reduced reliability. On the other hand, using a digital processor, the number of components is reduced, bringing high reliability and flexibility [7].

Predictive control has been successfully applied to power electronic devices such as three phase inverters [8]. The main advantages of this control method are a high dynamic response, simplicity, robustness and the capability of reach different and complex control objectives using the same software/hardware configuration [9]. Predictive control has been applied to several power converter topologies [10], and several cost functions have been proposed, like direct power control, flux and torque, and current frequency spectrum [11]. One of the drawbacks of this control scheme is the variable switching frequency, however, this topic has been covered in [12]. Considerations about the model [13] and algorithm implementation [14] have been recently addressed.

2 Current Control Methods for PFC Converters

In this section, a description of each proposed control method, its functional principle and features will be given. The current control has become a prominent method to control power electronic devices due to the continuous development of digital processing technologies. Current control methods are appropriate for systems that require tracking capabilities; hence they show high active response. Various current control methods have been proposed and classified as hysteresis control, predictive control and linear control. Principle of these methods are briefly described and discussed below.

2.1 Hysteresis Control

Hysteresis current control is an instantaneous feedback control system which uses the current error when exceeds the limit of the band, the switches are turned on/off. The advantage of this technique is simple, accurate, and robust. Also, the speed of the response is limited by switching speed of the device and time constant of the load. The variable switching frequency operation is considered as the only disadvantage.

2.2 Linear Control

In the linear control scheme, the actual currents are compared to the references and the errors are processed by conventional proportional-integral controllers to provide a reference control signal for a PWM modulator. This produces constant-frequency with pulse width-modulated gate signals for the converter switches. The controller parameters are adjusted to optimize the system transient

response. The implementation of linear controller is relatively straightforward using standard integrated circuits.

3 Boost Converter Topology in AC – DC Converter

The boost converter topology is used for controlling the output and input performance. Various current control strategies have been applied. The input current is maintained sinusoidal with unity power factor. The output voltage of AC to DC converter is regulated and maintained. The operation and controller implementation are discussed below to achieve the said performance.

Figure 1 shows a single-phase AC to DC converter, where a single-phase diode bridge and a following single ended boost converter are employed. An inductor L called the boost inductor is connected in series; the output capacitor C is connected in parallel to the load R reduces the ripple in the output voltage.

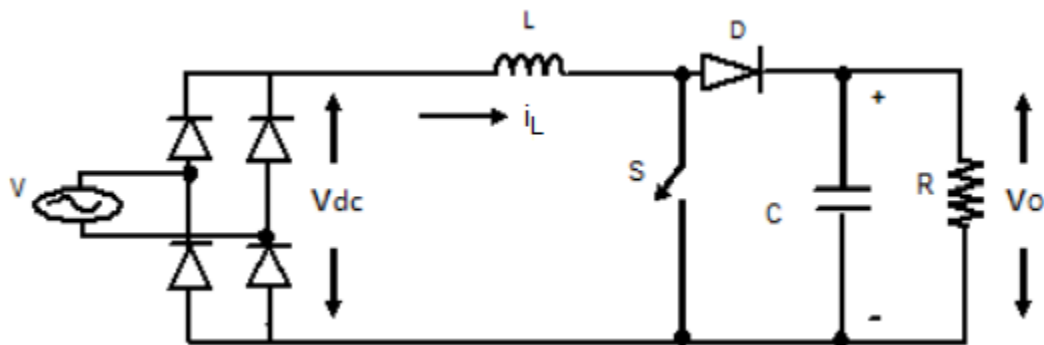


Figure 1 - Boost AC to DC Converter

By controlling the switch S , appropriately, the input current and output voltage are maintained at a desirable value and shape. The boost converter operates in two modes, which are mode ON and mode OFF. During mode ON, the switch S is in on state and hence, the diode is reverse biased. In this mode, source is short through L , Diode Bridge and switch S . As a result, the current in the inductor L increases. During mode off S is turned off. The diode D is forward biased. The source is connected to the capacitor C through bridge, the inductor L and the Diode D . As a result, the inductor current (i_L) decreases. The output voltage (V_o) gets increased and will become more than the V_{dc} .

This topology is cost effective due to single control switch. The number of conducting devices is three, i.e., the switch (s) and two diodes of the bridge conduct. The reverse recovery property of the diodes produces high switching losses and results in low efficiency.

3.1 Resistance, R, Inductance, L and Capacitance, C Design

For the given specification of the converter, procedure to design the value of R, L, and C is as follows. In general, current ripple is considered for designing the value of inductance L. Voltage ripple is considered for designing the value of capacitance C.

The maximum ripple current [$I_{rip\ max}$] for this converter is given as:

$$I_{rip\ max} = \frac{V}{4f_s L} \quad (1)$$

where V: Output Voltage

f_s : Switching Frequency

The voltage ripple (V_{ripple}) for this converter is given as:

$$V_{ripple} = \frac{1}{2\omega C} \quad (2)$$

where I: Output Current

C: Capacitance

4 Closed Loop Operation of Boost Converter Topology with Predictive Control

The predictive control predicts the current-error-vector at the beginning of each modulation period. The prediction is based on the error and the load variables. The predicted voltage vector is used by the PWM pulse generator during the next modulation cycle and hence minimizes the error. This technique uses more information along with regulator error signal and hence produces accurate output response from the converters. The predictive regulators are particularly suitable for digital implementation. Where the signal acquisition can be discrete and suitable for implementation in digital which may provide good calculation, power needed for effective control of the converter operation and improve the performance. The closed loop arrangement of the boost converter-based ac to dc converter topology with predictive control is shown in Figure 2 presented as follows.

The switch voltage reference $V_{sw\ ref}$ at $(k + 1)^{th}$ instant is predicted at k^{th} instant itself for the circuit shown in Figure (2) by means of Equation (4).

$$V_{sw\ ref}(k) = V_d(k) - L \{i_d(t_{k+1}) - i_d(t_k)\} / T \quad (3)$$

Where V_d : rectified voltage

i_d : inductor current

T: Modulation period (inverse of switching frequency)

To implement the Equation (3) all the parameters at the k^{th} instant can easily be sensed, except the current i_d at $(k + 1)^{th}$ instant. For that the reference signal i_d^* which has been derived from the rectified voltage as shown in Figure 2 has been phase shifted by a modulation period of $(t_{(k+1)} - t_k)$ and it has been used in the Equation (3) as $i_d^*(k + 1)$ instead of $i_d(k + 1)$. So, the control law has been modified as Equation (4)

$$V_{sw\ ref}(k) = V_d(k) - L \{i_d^*(t_{k+1}) - i_d(t_k)\} / T \quad (4)$$

Since the switching frequency is very high the modulation period is very small. The current i_d at $(k + 1)^{th}$ instant will be approximately equal to the current i_d at k^{th} instant. So, the Equation (4) is modified to (5).

$$V_{sw\ ref}(k) = V_d(k) - L \{i_d^*(t_k) - i_d(t_k)\} / T \quad (5)$$

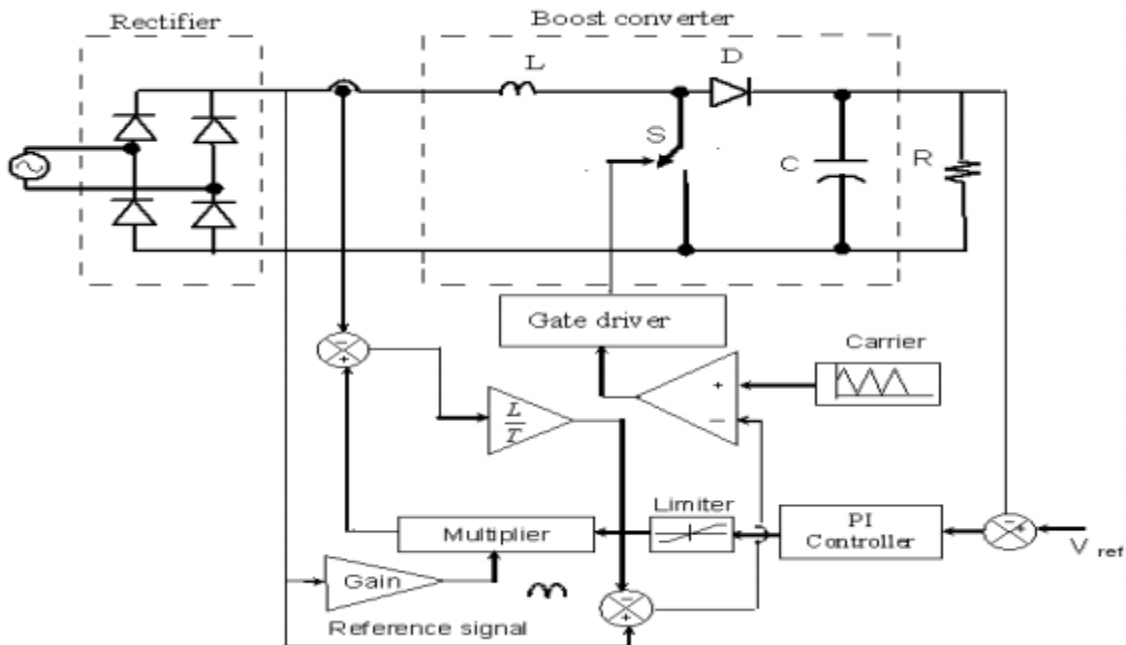


Figure 2 -Boost Converter with Predictive Control

The same control law has been written in Analog domain as Equation (5). It is implemented in the circuit shown in Figure 2 to obtain the reference switch voltage ($V_{sw\ ref}$).

$$V_{sw\ ref}(t) = V_d(t) - L \{i_d^*(t) - i_d(t)\} / T \quad (6)$$

The reference switch voltage is compared with the carrier whose amplitude is varying according to the load voltage and it is given to the switch S. The operation of the switch results in sinusoidal current and unity power factor. PI-controller has been used externally to regulate the output voltage.

5 Results and Discussion

Simulation is performed by MATLAB to verify the proposed digital PFC control strategy. The results presented in Figures (3) – (11) validate the predictive control strategy in power factor correction for the specifications given in Table 1. Figure (3) is the input current and voltage of the PFC Boost circuit under 100 W load (full-load) with 9 A and 55 V (RMS) input voltage respectively. The corresponding harmonics of the input current is shown in Figure (4) and it can be seen that the 3rd harmonic is at a value slightly below 4% of the fundamental, with a THD of 4.48%. The predictive PFC control strategy can achieve very high power factor (0.997) at full-load.

The dynamic performance is also verified by simulation. The input and output voltage and current waveforms, and THD in transient state in which the load is changed from 50% load to full-load are shown in Figures (6) – (8). At steady state, it is observed that the THD is slightly lower than 4.49% at full-load (4.48%) and the PF is 0.992. The transient is quite swift and occurs in a split second as shown in Figure (8) for the output current, however the voltage remained fairly the same.

Table 1 Converter Specifications Used

Source Voltage	55 V (rms)
Output Voltage	100 V (avg)
Output Power	100 W
Capacitance	2 mF
Inductance	1.5 mH
Line Current THD	≤ 5 %
Switching Frequency	160 kHz

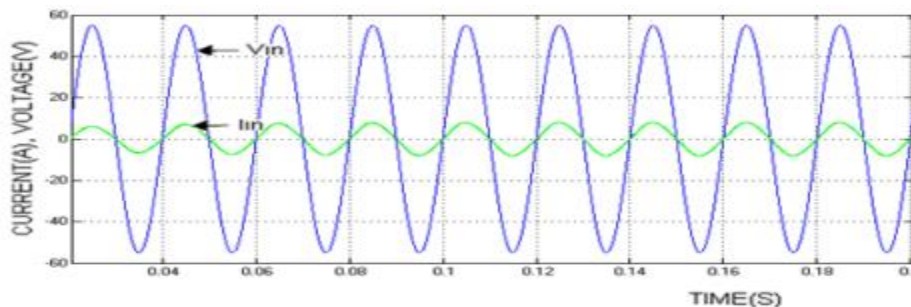


Figure 3 - Input Current and Voltage Waveform at Full Load (100W)

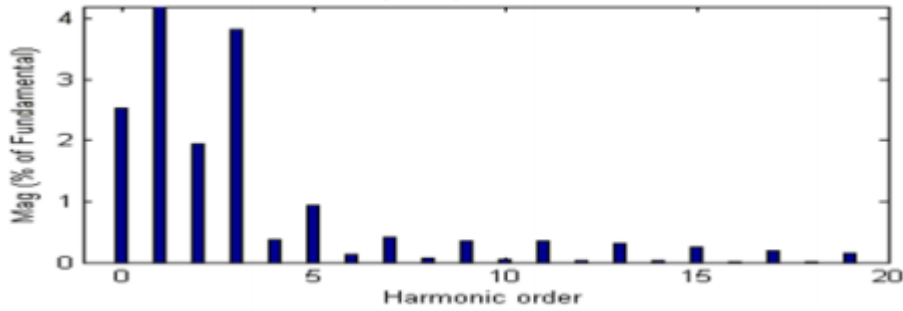


Figure 4 - Harmonic Spectrum of Input Current at Full Load (100W) Fundamental (50Hz) = 6.215, THD = 4.48%

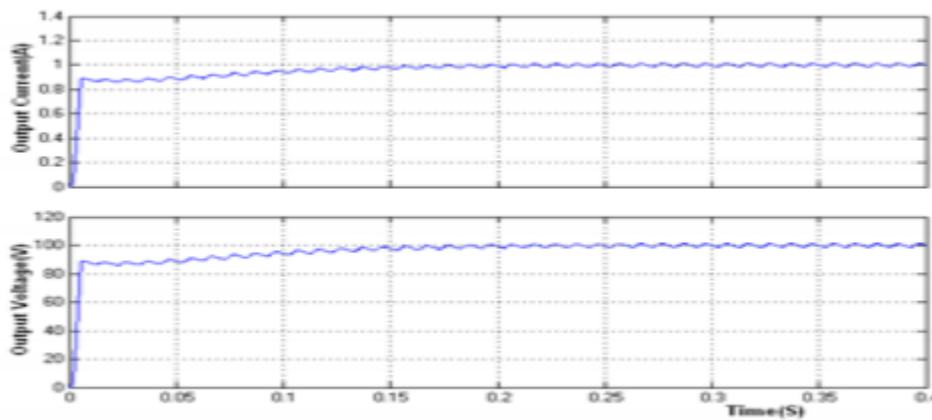


Figure 5 - Output Current and Voltage Waveform at Full Load (100W)

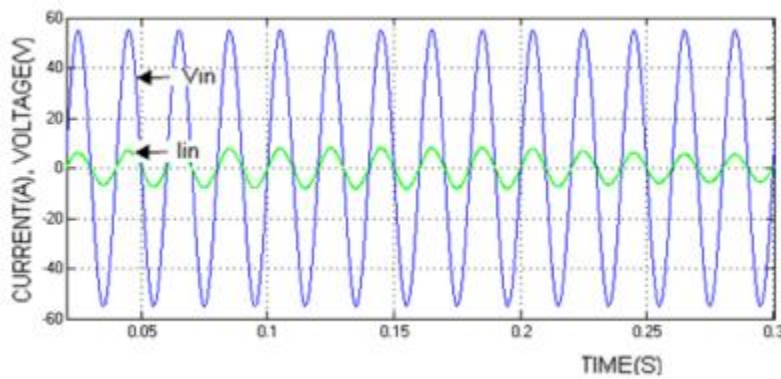


Figure 6 - Input Voltage and Current Waveform in transient state

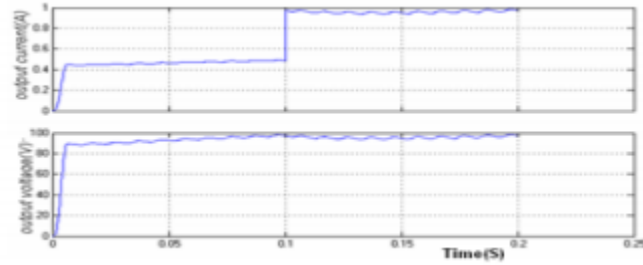


Figure 7 - Output Current and Voltage in transient state

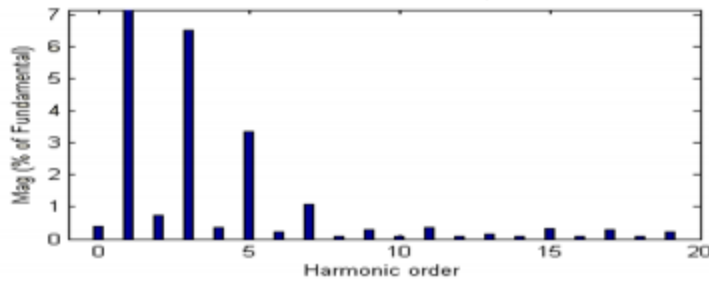


Figure 8 - Harmonic Spectrum of input current in transient state Fundamental (50Hz) = 4.323, THD = 4.49%

A distorted input test was also carried out on the system. Figure (9) shows the input voltage and current plots for a distorted input. It can be seen that the voltage sinusoid is not constant but distorted, however, the current is fairly the same throughout. The results for the output voltage and current and the THD spectrum at full load are given in Figures (10) and (11). Table 2 summarizes the values of the power factor and THD obtained for the different cases and it can be seen that the power factor is relatively high and the THD is below 5% except for the case of the distorted input.

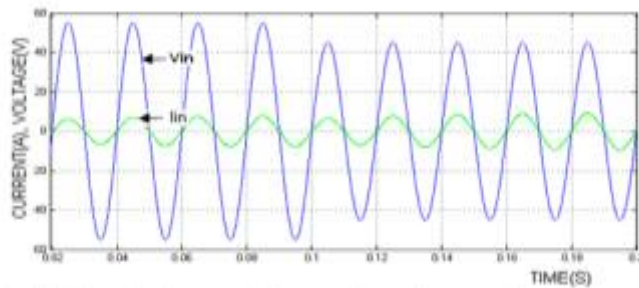


Figure 9 - Input Voltage and Current Waveform at Distorted Input

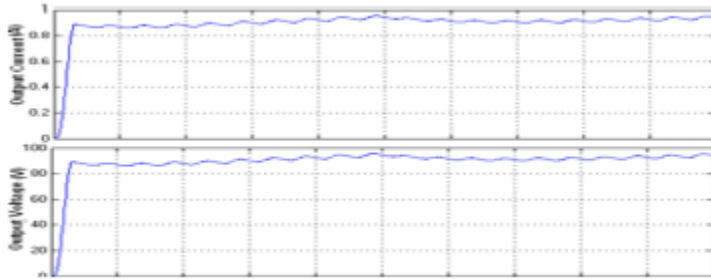


Figure 10 - Output Current and Voltage at Distorted Input

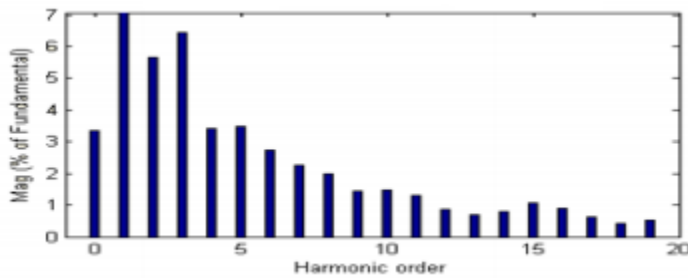


Figure 11 - Harmonic Spectrum of input current at Distorted Input Fundamental (50Hz) = 4.051, THD = 5.16%

Table 2 Output Voltage, Power Factor and THD for Different Cases

Case	Output Voltage (V)	Power Factor	% Total Harmonic Distortion
Full Load	100	0.997	4.48
Transient state	99.5	0.992	4.49
Distorted Input	99.5	0.998	5.16

6 Conclusion

Simulation was used to investigate and verify the closed loop efficiency of PFC converters with predictive control schemes. The suggested approach performs well in simulations, and near to unity power factor can be obtained over a large range of input voltage and load variations. For phase load change and input voltage transition, the proposed PFC control strategy will achieve sinusoidal current waveform in the transient state. The power factor is held near unity (0.99), and the THD in the input current is $\leq 5\%$. Regardless of load and supply voltage variations, the output voltage is kept constant at 100V.

Conflict of Interest

There is no conflict of interest associated with this work.

References

- [1] B.-R. Lin and H.-H. Lu, "Single-phase power-factor-correction AC/DC converters with three PWM control schemes," *IEEE Transactions on Aerospace and Electronic Systems*, vol. 36, no. 1, pp. 189–200, Jan. 2000.
- [2] D. G. Lamar, A. Fernandez, M. Arias, M. Rodriguez, J. Sebastian, and M. M. Hernando, "A unity power factor correction preregulator with fast dynamic response based on a low-cost microcontroller," *IEEE Transactions on Power Electronics*, vol. 23, no. 2, pp. 635–642, Mar. 2008.
- [3] M. Chen, A. Mathew, and J. Sun, "Nonlinear current control of single-phase PFC converters," *IEEE Transactions on Power Electronics*, vol. 22, no. 6, pp. 2187–2194, Nov. 2007.
- [4] J.-F. Chen, R.-Y. Chen, and T.-J. Liang, "Study and implementation of a single-stage current-fed boost PFC converter with ZCS for high voltage applications," *IEEE Transactions on Power Electronics*, vol. 23, no. 1, pp. 379–386, Jan. 2008.
- [5] F. Ö. Alkurt, M. Bağmancı, and M. Karaaslan, "Design of a Dual Band Metamaterial Absorber for Wi-Fi Bands," in *AIP Conference Proceedings*, 2018, vol. 1935, pp. 1–5, doi: 10.1063/1.5025979.
- [6] W. Chen, C. M. Bingham, K. M. Mak, N. W. Caira, and W. J. Padilla, "Extremely subwavelength planar magnetic metamaterials," vol. 201104, pp. 1–5, 2012, doi: 10.1103/PhysRevB.85.201104.
- [7] Y. Zhu, X. Fan, B. Liang, J. Cheng, and Y. Jing, "Ultrathin Acoustic Metasurface-Based Schroeder Diffuser," *Phys. Rev. X*, vol. 7, no. 2, pp. 1–11, 2017, doi: 10.1103/PhysRevX.7.021034.
- [8] W. Xu and S. Sonkusale, "Microwave diode switchable metamaterial reflector / absorber Microwave diode switchable metamaterial reflector / absorber," *Appl. Phys. Lett.*, vol. 103, no. 3, pp. 3–7, 2013, doi: 10.1063/1.4813750.
- [9] F. Ding, Y. Cui, X. Ge, Y. Jin, and S. He, "Ultra-Broadband Microwave Metamaterial Absorber," *Appl. Phys. Lett.*, vol. 100, no. 10, 2012, doi: 10.1063/1.3692178.
- [10] Q. Wen, H. Zhang, Y. Xie, Q. Yang, and Y. Liu, "Dual band terahertz metamaterial absorber: Design, fabrication, and characterization," *Appl. Phys. Lett.*, vol. 95, no. 24, 2009, doi: 10.1063/1.3276072.
- [11] Y. Huang, X. Yuan, C. Wang, M. Chen, L. Tang, and D. Fang, "Flexible thin broadband microwave absorber based on a pyramidal periodic structure of lossy composite," *Opt. Lett.*, vol. 43, no. 12, pp. 2764–2767, 2018.
- [12] M. B. Abdullahi and M. H. Ali, "Design and Simulation of Cross-Block Structured Radar Absorbing Metamaterial Based on Carbonyl Iron Powder Composite," *Niger. J. Technol.*, vol. 38, no. 4, pp. 912–918, 2019.
- [13] D. Zhou, X. Huang, Z. Du, and Q. Wang, "Calculation and Analysis of the Effective Electromagnetic Parameters of Periodic Structural Radar Absorbing Material Using Simulation and Inversion Methods," vol. 52, no. October, pp. 57–66, 2016.
- [14] N. Dib, M. Asi, and A. Sabbah, "On the optimal design of multilayer microwave absorbers," *Prog. Electromagnet. Res. C*, vol. 13, pp. 171–185, 2010, doi: 10.2528/PIERC10041310.